MD-Vol. 68/AMD-Vol. 215, Mechanics of Plastics and
Plastic Composites
ASME 1995

PRELIMINARY RESULTS ON AN EFFORT TO CHARACTERIZE THERMO-MECHANICAL RESPONSE OF AMORPHOUS POLYMERS IN THE GLASS-TRANSITION RANGE

Mehrdad Negahban
Department of Engineering Mechanics and
The Center for Materials Research and Analysis
University of Nebraska
Lincoln, NE 68588-0347

ABSTRACT

A theoretical structure is proposed to characterize the thermo-mechanical response of solid polymers at temperatures close to the glass transition. This structure is first developed in a one dimensional setting for shear, and constrained to satisfy the entropy production inequality. This results in expressions for shear stress, entropy, and an inequality constraint. A model is developed for each of the constitutive functions needed to characterize the shear response, and it is shown that the model can quantitatively reproduce the experimental response for a complex sequence of loading and unloading histories. The article concludes by providing the multidimensional counterpart for the proposed structure developed for shear.

1 Introduction

The behavior of polymers around the glass-transition temperature is both interesting and may contain clues for modeling polymer behavior in the non-equilibrium state of the polymer below the glass-transition temperature. One of the most fascinating phenomena observed in amorphous polymers is the recovery of large plastic strains by simply heating the polymer to within the glass-transition range. This delayed rubber-band like response is not only important in defining the behavior of the polymer, but also may be used in developing a variety of "smart" products and processing techniques.

The current article deals with a preliminary study of a sequence of experiments conducted on a cross-linked poly(methyl methacrylate) (PMMA). The material, as received from Pilkington Aerospace, was in a bi-axially stretched sheet form, which we annealed

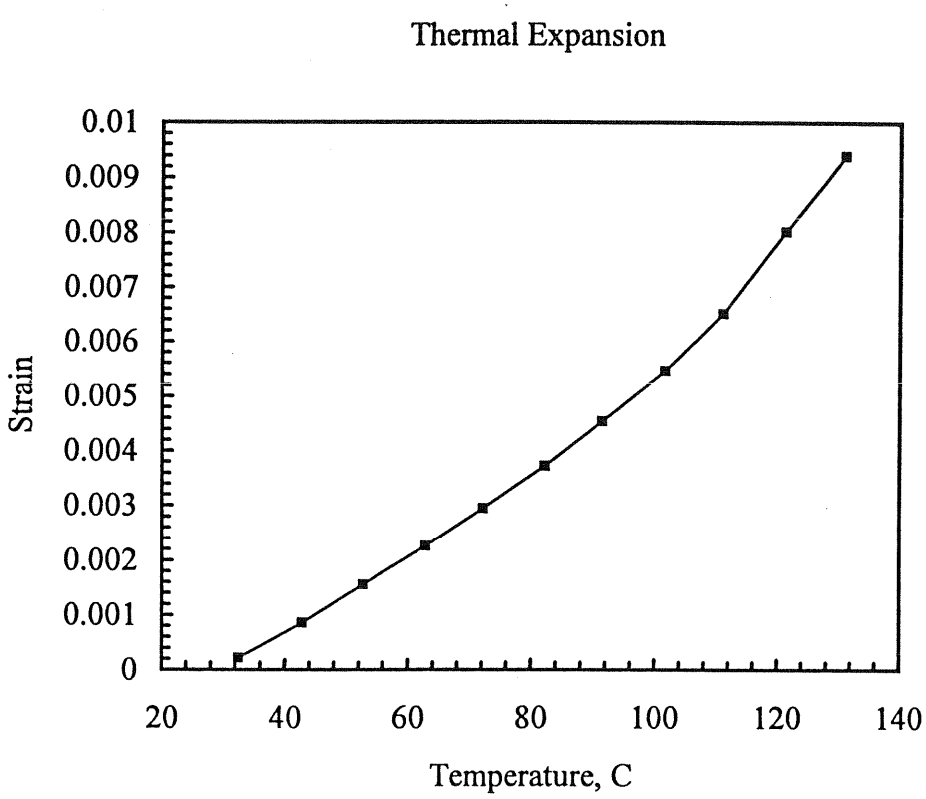

Figure 1: Thermal expansion of the PMMA during cooling at a rate of about 20°C per day.

at about 150°C for about a day and then oven cooled to room temperature. As a result of this annealing, the sheet shrunk to about 60% of its original dimensions and became about three times thicker. In spite of these large changes, the originally rectangular block retained its rectangular shape. Subsequent to this processing, test specimens were cut from the prepared block. These specimens were tested at several temperatures and under different loading conditions. The glass-transition temperature for this material was determined to be about 100°C, as evaluated from the thermal expansion of the annealed material (shown in Figure 1).

The focus of this article will be to develop a theoretical structure for modeling the behavior observed in a single shear experiment which consisted of a sequence of cycles, each containing a rapid loading and very slow unloading. This modeling will be done first by developing a one dimensional theory for shear and evaluating the constitutive functions from the first loading/unloading cycle, and later predicting the response over several cycles. Next, this model will be used to predict the observed response in a slightly different loading experiment. In both cases the predicted stress is in good agreement with the observed response.

The shear experiment under consideration is described by the strain history given in Figure 2, and the corresponding stress history given in Figure 3. The loading process occurred within an interval of two to three seconds, while the unloading occurred over a period of 10 to 15 hours. The process is further complicated by the lack of sufficient rigidity in the testing facility. This results in a region of further shearing of the sample even after the motion of the controlling arm is reversed. Figure 4 shows the stress-strain diagram for this experiment, where the initial increase in the strain during unloading is clearly shown. Over the entire interval of the experiment the temperature around the sample was kept to within ± 0.5°C of the stated temperature, as recorded by a

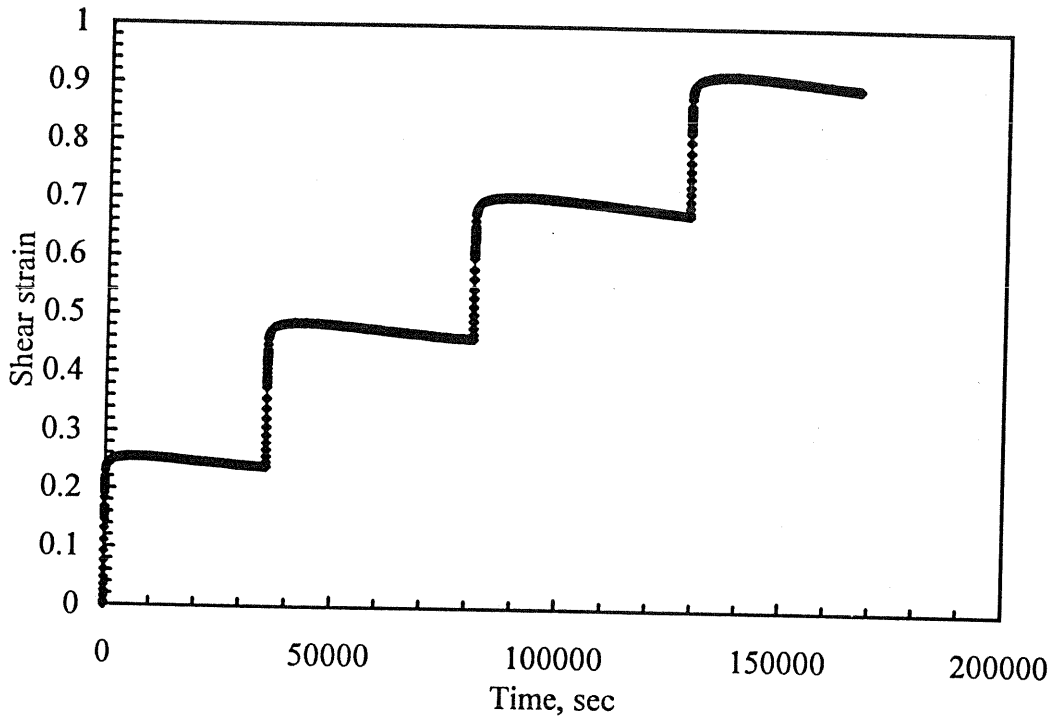

Figure 2: Shear strain history.

thermocouple. The load was measured by a load cell connected to the actuating arm. The shear was measured by an LVDT connected between the shearing surfaces.

The modeling is based on a structure similar to that used in plasticity, and recently exploited for capturing the behavior of polymers by Boyce and her co-workers (Boyce et al., 1988, 1989, 1990, and Arruda et al., 1995). The most prominent difference is the thermodynamic platform of the current work.

To study the experimental results and to develop the basic ideas needed to model the observed behavior, a one dimensional model will first be developed. Later in this article a full multidimensional model will be proposed which includes the ideas developed in the one dimensional model, in addition to some others which are specific to multidimensional theories.

2 A Model Specifically for Shear

Some of the basic ideas which are later used to develop a multidimensional model are easier understood in a one dimensional setting. In this section these ideas will be explored in the context of a model specifically developed to study shear. As will be shown, by using this one dimensional model one can study with much greater ease some of the relations between theory and experiment which become much more difficult in the multidimensional setting.

It will be assumed that during any process the only measurable kinematic parameter will be the shear strain γ. Temperature θ will be the only other independent variable. The plastic shear strain γ^p will be the only internal variable used, and is the strain at zero stress.

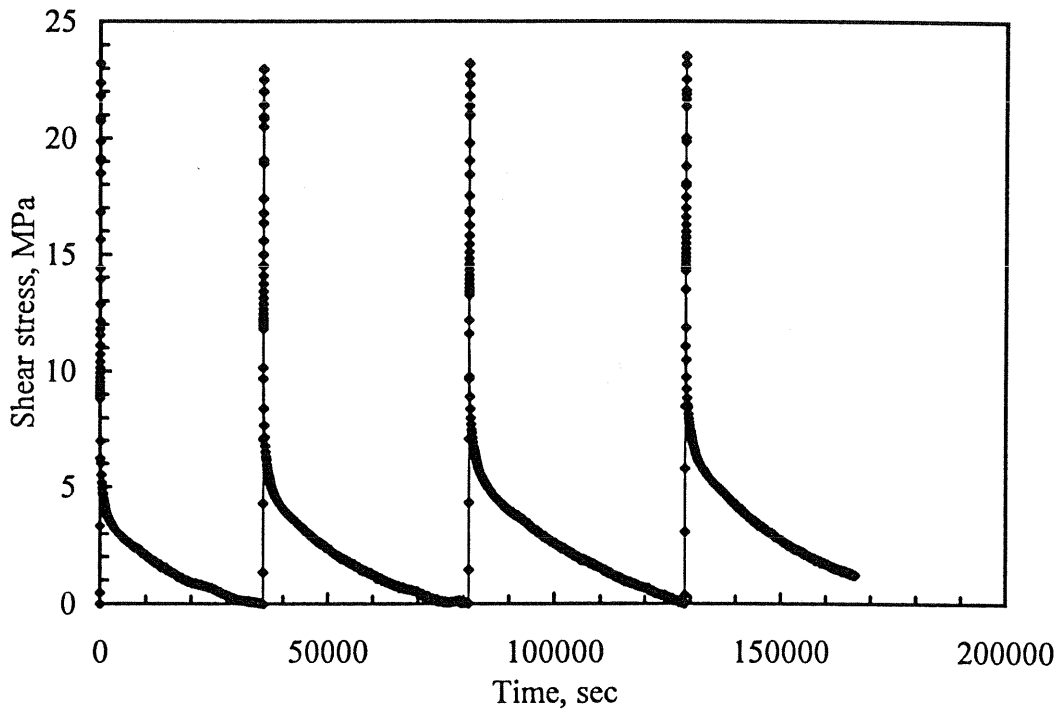

Figure 3: Shear stress history.

The dependent variables will be free-energy density ψ, shear stress τ, and entropy density η, all three assumed to be functions of our two independent variables and plastic strain. This will be denoted by

$$\psi = \psi^{\dagger}(\gamma, \gamma^p, \theta), \quad \tau = \tau^{\dagger}(\gamma, \gamma^p, \theta), \quad and \quad \eta = \eta^{\dagger}(\gamma, \gamma^p, \theta), \tag{1}$$

where a superscript "†" will denote the function or functional for a variable. The process is going to be assumed homogeneous, and as a result heat flux will be eliminated from consideration.

The entropy production inequality will be taken as

$$\rho\dot{\psi} - \tau\dot{\gamma} + \rho\eta\dot{\theta} \leq 0, \tag{2}$$

where ρ is density, and it is taken to be a function of temperature. Substituting the above constitutive assumption for free-energy density, one obtains

$$[\rho\frac{\partial\psi}{\partial\gamma} - \tau]\dot{\gamma} + \rho[\eta + \frac{\partial\psi}{\partial\theta}]\dot{\theta} + \rho\frac{\partial\psi}{\partial\gamma^p}\dot{\gamma}^p \leq 0. \tag{3}$$

This must hold for all possible processes. To manipulate this restriction and obtain relations between the unknown functions, one needs to establish the independence of the different terms of this equation. This can only be done after the establishment of an evolution equation ("flow rule") for the internal parameter γ^p.

The evolution equation for the internal parameter γ^p will be assumed to be given by the following relation

$$\dot{\gamma}^p = A_1\dot{\gamma} + A_2\dot{\theta} + A_3, \tag{4}$$

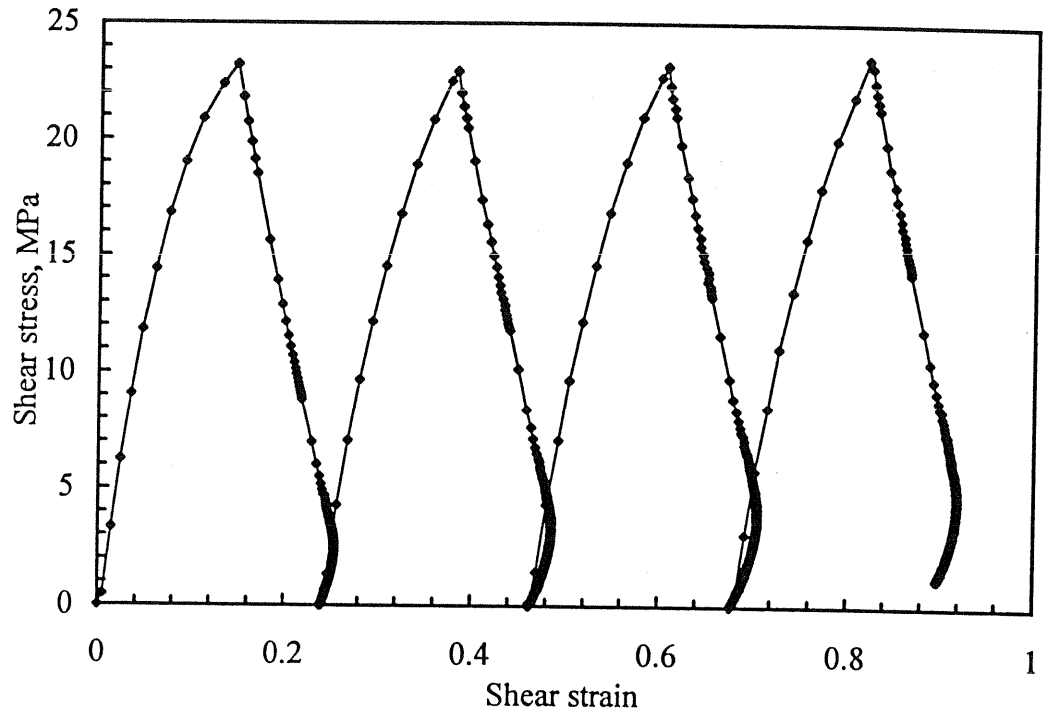

Figure 4: Stress-strain diagram for the response shown in Figures 2 and 3.

where

$$A_i = A_i^{\dagger}(\gamma, \gamma^p, \theta). \tag{5}$$

As a result of the fact that this flow rule cannot be made time independent, a rate dependence will appear in the final response. This will be discussed later.

The first main departure from classical plasticity is the fact that there is no yield condition or yield function; this follows the ideas of Boyce et al. (1988).

For the given flow rule, the entropy production inequality can be rewritten as

$$[\rho(\frac{\partial \psi}{\partial \gamma} + A_1 \frac{\partial \psi}{\partial \gamma^p}) - \tau]\dot{\gamma} + \rho[\eta + \frac{\partial \psi}{\partial \theta} + A_2 \frac{\partial \psi}{\partial \gamma^p}]\dot{\theta} + \rho \frac{\partial \psi}{\partial \gamma^p} A_3 \leq 0, \tag{6}$$

where the three terms in this equation can now be considered independent. This results from an implied assumption that in theory one can select the rate of change of strain and the rate of change of temperature independently, and each may take any arbitrary value. Under this assumption, the only way to satisfy the inequality is that the following relations always be satisfied. These relations are:

$$\tau = \rho(\frac{\partial \psi}{\partial \gamma} + A_1 \frac{\partial \psi}{\partial \gamma^p}), \tag{7}$$

$$\eta = -\frac{\partial \psi}{\partial \theta} - A_2 \frac{\partial \psi}{\partial \gamma^p}, \tag{8}$$

and

$$A_3 \frac{\partial \psi}{\partial \gamma^p} \leq 0. \tag{9}$$

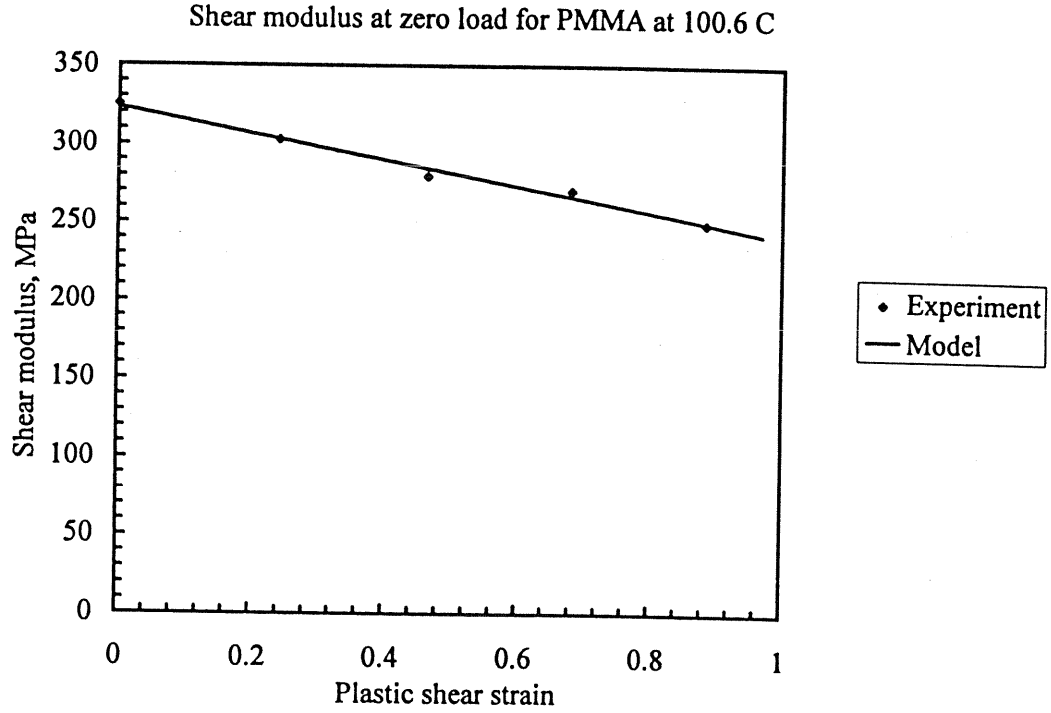

Figure 5: Shear modulus as a function of plastic strain as evaluated from the experimental data and as evaluated from equation (15).

The second main departure from classical plasticity will be in the selection of a more specific form of the free-energy. The free-energy density will be assumed to be a sum of two parts. One part which is readily available and another which drives the long term delayed response. This will be written as

$$\psi = \psi^e + \psi^b, \tag{10}$$

where ψ^e is the more readily available part and will be associated with the "elastic response," and ψ^b will be associated with the delayed response (a back stress). The functional dependence of these are specified by

$$\psi^e = \psi^{e\dagger}(\gamma, \gamma^p, \theta) \quad and \quad \psi^b = \psi^{b\dagger}(\gamma^p, \theta). \tag{11}$$

Substitution into the expression for the shear stress results in

$$\tau = \rho(\frac{\partial \psi^e}{\partial \gamma} + A_1 \frac{\partial \psi^e}{\partial \gamma^p} + A_1 \frac{\partial \psi^b}{\partial \gamma^p}). \tag{12}$$

It is immediately evident that in this model the shear stress is not only a derivative of the elastic part, but also has a term associated with the delayed response. The last two terms will be eliminated if A_1 vanishes, which happens when the plastic strain rate is not a function of the strain rate. The experimental data does suggest that this is the case for small stresses.

For the remainder of this section attention will be focused on isothermal response. As a result, $\dot{\theta}$ will be set to zero.

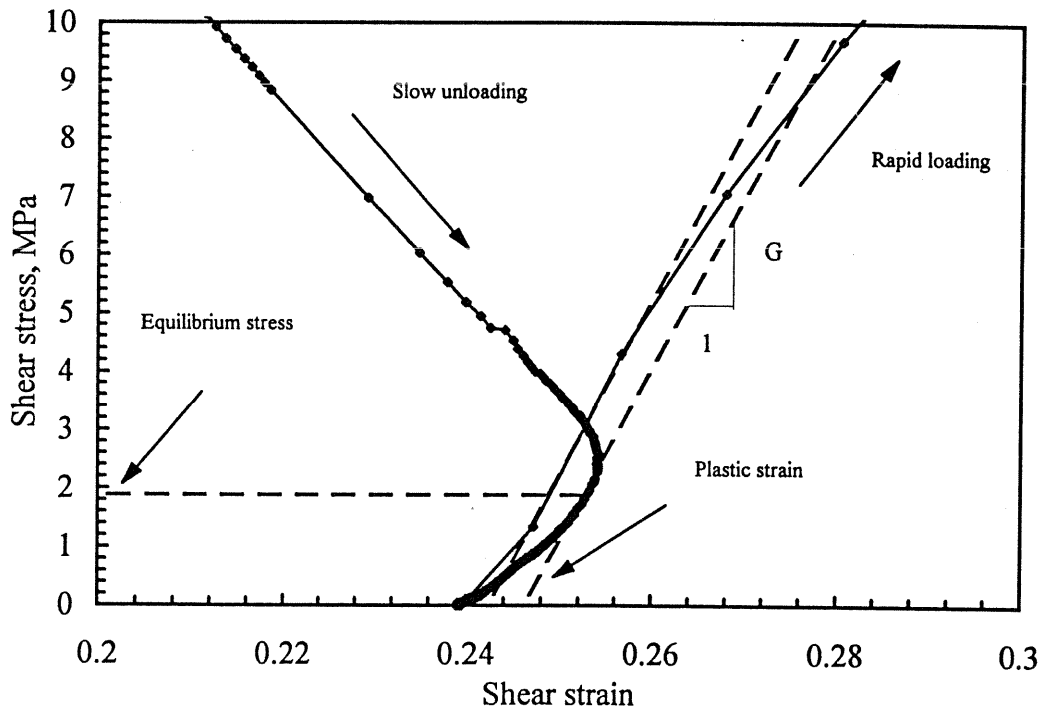

Figure 6: The method of evaluating the shear modulus G, the equilibrium stress, the corresponding plastic strain.

The elastic response is very close to linear in nature, in part a result of the small elastic strains involved. The simplest model compatible with the observed response is given by a free-energy of the form

$$\psi^e = \frac{G}{2\rho}(\gamma - \gamma^p)^2, \tag{13}$$

where G is a function of temperature and plastic strain. As stated above, the data suggests that close to zero load A_1 goes to zero, and therefore under these conditions one may evaluate the stress from

$$\tau = G(\gamma - \gamma^p). \tag{14}$$

The shear modulus G can be taken from the stress-strain diagram by evaluating the slope of the stress-strain curve at stresses close to zero and for sufficiently rapid loading such that γ^p can be taken constant. Note that even though A_1 is taken to be zero around zero load, A_3 is not zero, and if the loading is slow it will contribute substantially to the change in stress. Figure 4 shows our typical stress-strain response which includes loading and unloading for our test material. Figure 5 shows G as a function of plastic strain for this same material. An appropriate model for G is

$$G = G_o - G_1|\gamma^p|, \tag{15}$$

where G_o and G_1 are functions of temperature and given at 100.6°C as

$$G_o = 323\ MPa \quad and \quad G_1 = 82\ MPa. \tag{16}$$

Another point of interest happens when $\frac{\partial \psi}{\partial \gamma^p}$ changes sign. If this function and the function for A_3 are continuous, as $\frac{\partial \psi}{\partial \gamma^p}$ passes through zero the entropy production inequality requires that A_3 also pass through zero and change sign. This follows from

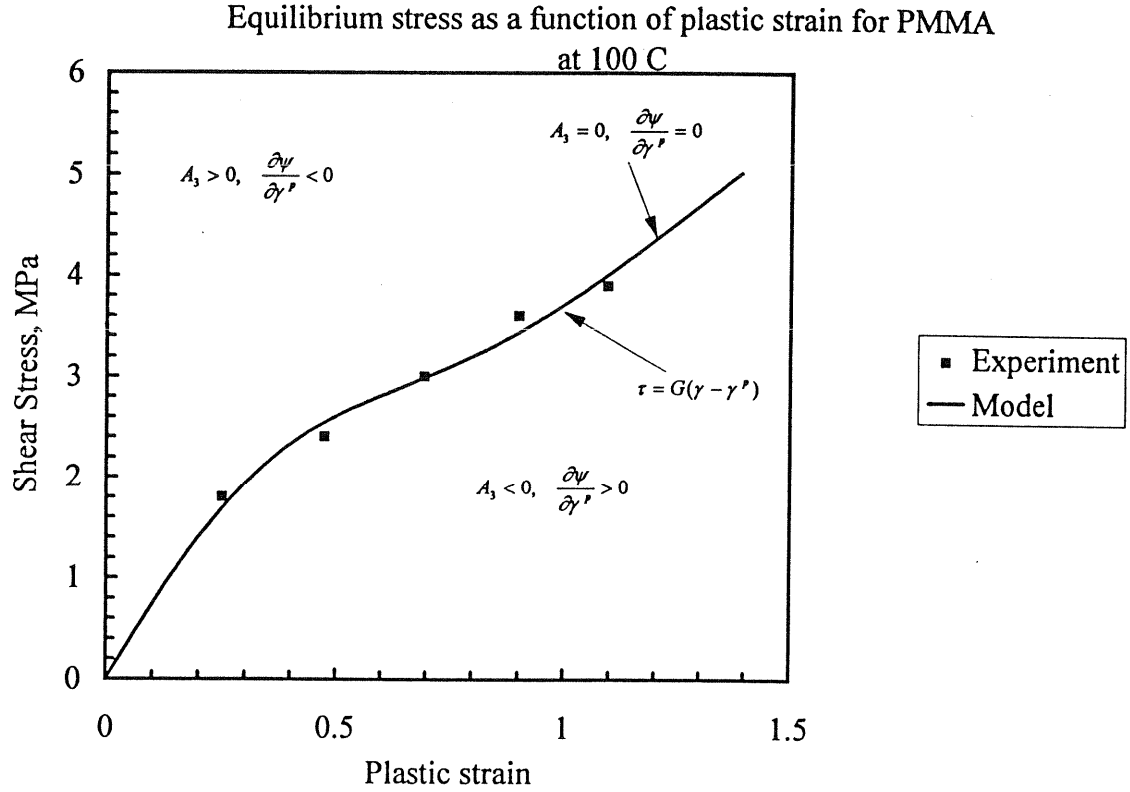

Figure 7: The equilibrium stress as a function of plastic strain as evaluated from the data and from the equation (19).

constraint (9) imposed by the entropy production inequality. Therefore, at $\frac{\partial \psi}{\partial \gamma^p} = 0$ one must have $A_3 = 0$. Also, the expression for shear stress becomes $\tau = G(\gamma - \gamma^p)$ due to the elimination of the second term in (7). The stress rate at this point becomes

$$\dot{\tau} = G[1 - 2A_1(1 - \frac{1}{G^2}\frac{\partial G}{\partial \gamma^p}\tau) + A_1^2(1 - \frac{2}{G^2}\frac{\partial G}{\partial \gamma^p}\tau + \frac{1}{2G^3}\frac{\partial^2 G}{\partial \gamma^{p2}}\tau^2) + \frac{A_1^2}{G}\rho\frac{\partial^2 \psi^b}{\partial \gamma^{p2}}]\dot{\gamma}. \quad (17)$$

Since the stress is small relative to the shear modulus and also since the modulus of the equilibrium response is much smaller than the rapid response, one can approximate this relation with good accuracy by the relation

$$\dot{\tau} = G(1 - A_1)^2\dot{\gamma}. \quad (18)$$

Since A_1 should be small at small loads, the set of points which have $\frac{\partial \psi}{\partial \gamma^p} = 0$ and $A_3 = 0$ can be approximated by finding the points of slope G on a sequence of slow loading or unloading processes. Figure 6 shows how the equilibrium points were evaluated from the data. The stress and corresponding plastic strain at $\dot{\gamma}^p = 0$ are shown in Figure 7. This figure also shows a fit to this data obtained by using the equation

$$\tau^{eq} = (G_o^{eq} + G_1^{eq}e^{-k\gamma^{p2}})\gamma^p, \quad (19)$$

where τ^{eq} designates the equilibrium stress (the stress at which for very slow strain rates $\dot{\gamma}^p = 0$), and the evaluated constants at 100.6°C are given as

$$G_o^{eq} = 3.6MPa, \quad G_1^{eq} = 4.0MPa, \quad k = 3.6. \quad (20)$$

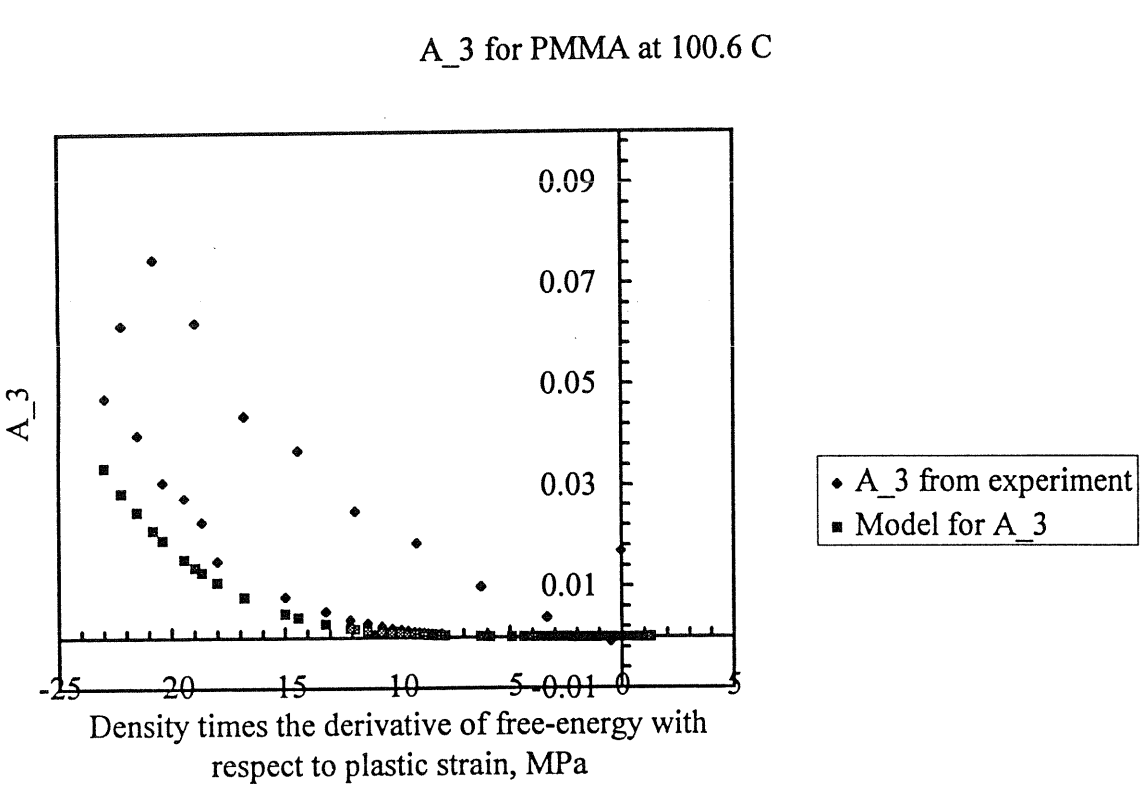

Figure 8: A_3 as evaluated from the first loading unloading cycle, and as evaluated from equation (24).

As stated above, the entropy production inequality constrains the response. That is, as one moves from one side of the equilibrium response curve to the other, the signs of A_3 and $\partial\psi/\partial\gamma^p$ change, and on the equilibrium response curve both A_3 and $\partial\psi/\partial\gamma^p$ have zero value resulting in the relation $\tau = \rho\partial\psi^e/\partial\gamma$. These relations are illustrated on Figure 7.

The process used to evaluate the equilibrium stress assumes that A_1 is very small so that the term $(1 - A_1)^2$ in (18) can be approximated as being equal to unity. Since A_1 should be greater than zero and smaller than unity, the evaluated equilibrium stress should be larger than the actual equilibrium stress. The error introduced by the assumption that A_1 is small is not totally negligible. To capture this effect, in the remainder of the article an equilibrium stress equal to 80% of the above value is used.

The requirement that $\frac{\partial\psi}{\partial\gamma^p} = 0$ at equilibrium provides a means of calculating $\frac{\partial\psi^b}{\partial\gamma^p}$. This process results in

$$\rho\frac{\partial\psi^b}{\partial\gamma^p} = \tau^{eq} - \frac{1}{2G^2}\frac{\partial G}{\partial\gamma^p}\tau^{eq2}. \tag{21}$$

No attention has yet been given to evaluating the functions A_1 and A_3 needed for determining $\dot{\gamma}^p$, other than determining the set of points at which $A_3 = 0$ (the equilibrium points). The strategy will be to first evaluate A_3 based on the assumption that $A_1 = 0$ at all points. This should be a good assumption under slow loading and at small stresses. This assumption in isothermal processes gives the relation

$$\dot{\tau} = \rho[\frac{\partial^2\psi^e}{\partial\gamma^2}\dot{\gamma} + \frac{\partial^2\psi^e}{\partial\gamma^p\partial\gamma}\dot{\gamma}^p], \tag{22}$$

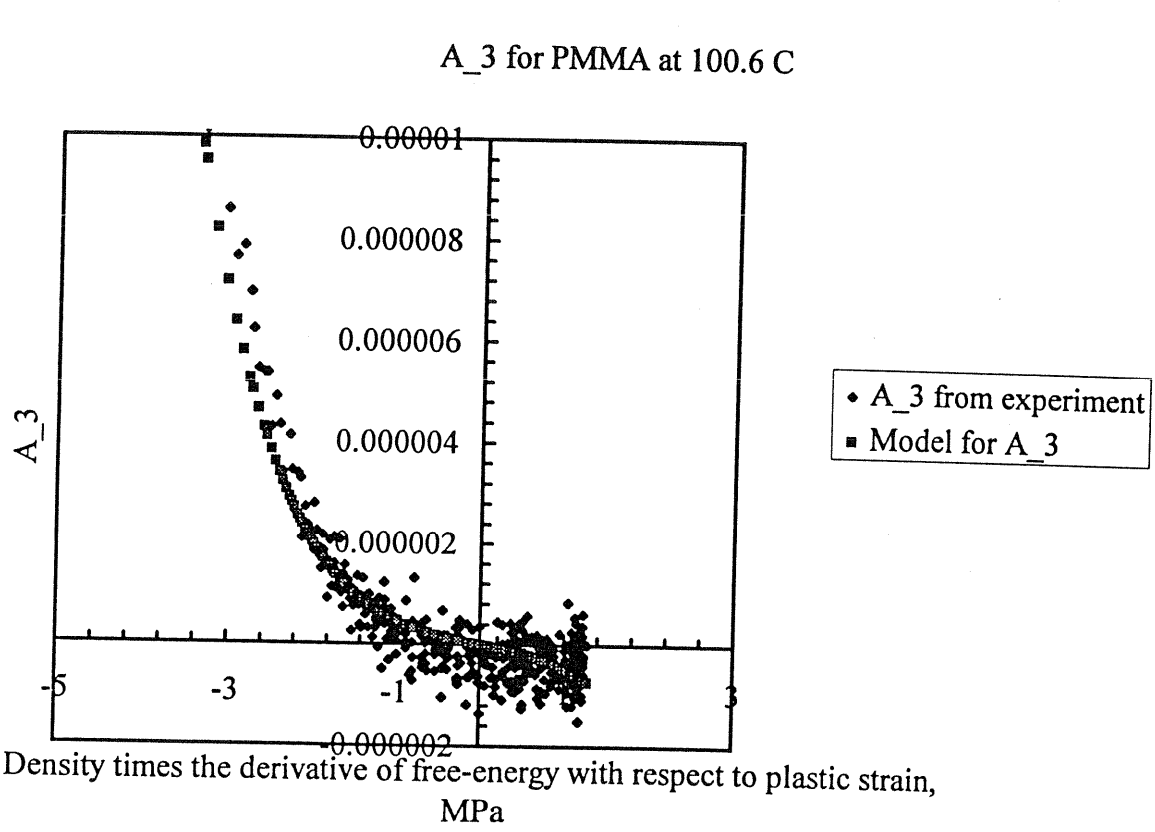

Figure 9: Expanded view of Figure 8.

which can be used with the relation $\dot{\gamma}^p = A_3$ to find A_3 from

$$A_3 = \frac{\dot{\tau} - G\dot{\gamma}}{\frac{\tau}{G}\frac{\partial G}{\partial \gamma^p} - G}. \tag{23}$$

Since τ, $\dot{\tau}$, and $\dot{\gamma}$ are directly available from the experiment, and since we have already evaluated G, it is possible to extract an approximation of A_3 from the experiment. Figure 8 shows A_3 as evaluated from the first cycle of the experimental data by using this method and presented as a function of $\rho\frac{\partial \psi}{\partial \gamma^p}$, and also A_3 as evaluated from equation

$$A_3 = -A_{3_0}(1 + A_{3_1}|\rho\frac{\partial \psi}{\partial \gamma^p}| + A_{3_2}|\rho\frac{\partial \psi}{\partial \gamma^p}|^2 + A_{3_3}|\rho\frac{\partial \psi}{\partial \gamma^p}|^3 + ...)\rho\frac{\partial \psi}{\partial \gamma^p}, \tag{24}$$

for appropriate constants A_{3_0}, A_{3_1}, ... Figure 9 shows the portion of Figure 8 around the origin, indicating the model function reproduces the behavior at all scales of the response.

A point to note in Figure 8 is that A_3 as calculated from the experimental data is not single valued. The model proposed in (24) is used only to model the lower curve which represents points during the slow unloading. The discrepancy between the lower curve and upper curve will be accounted for by A_1. It should also be noted that without A_1 the model would have no way to account for this discrepancy. In addition, as one moves towards the larger negative values of $\rho\partial\psi/\partial\gamma^p$, the effect on A_1 becomes more important due to the rapid nature of the response. The deviation of the model from the experiment is, therefore, not of concern in this range.

The form of A_1 can now be studied using the model proposed for A_3. For our experi-

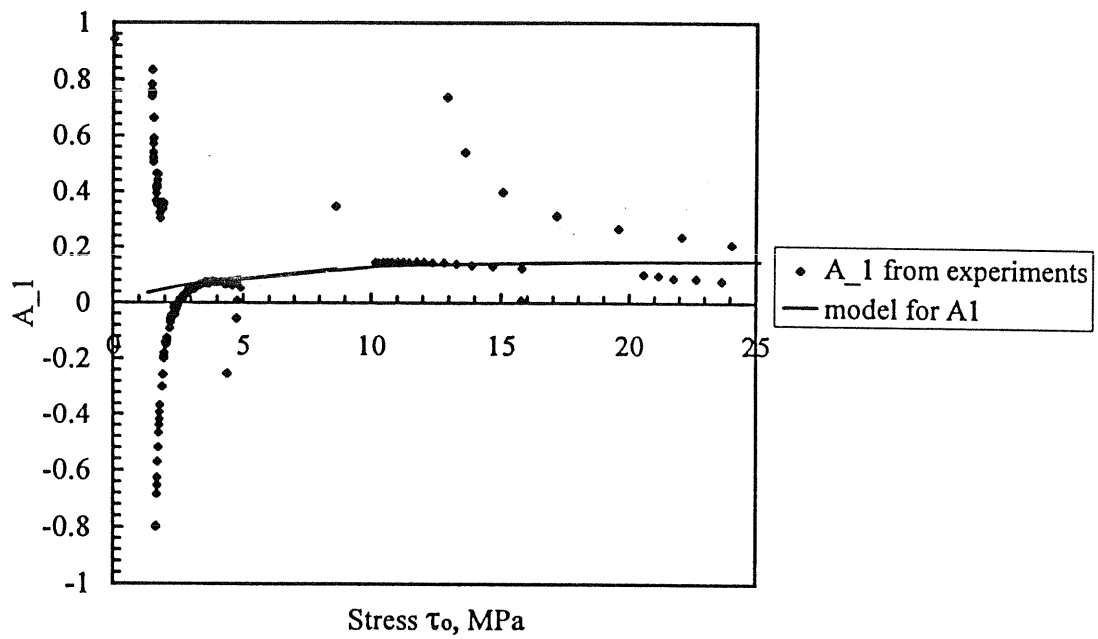

Figure 10: A_1 as evaluated from the first cycle of the experiment, and as evaluated from equation (26).

mental data, this is done by using the relation

$$A_1 = \frac{\tau - \rho \frac{\partial \psi^e}{\partial \gamma}}{\rho \frac{\partial \psi}{\partial \gamma^p}}, \tag{25}$$

which results from equation (7). This process yields Figure 10 which gives A_1 with respect to $\tau_o = G(\gamma - \gamma^p)$. This figure also shows the function

$$A_1 = A_{1_o}[1 - e^{-m|\gamma - \gamma^p|}], \tag{26}$$

which will be used to model A_1. It must be noted that the method of obtaining A_1 from the data takes A_1 to infinity when $\partial\psi/\partial\gamma^p$ passes through zero. This happens as one moves through the equilibrium stress, resulting in the vertical asymptotes in Figure 10. This portion should be disregarded in the modeling.

At this point the proposed procedure has provided the first approximations for G, A_1, A_3, and τ^{eq}. Figure 11 shows the experimental value of τ as a function of γ, and the predicted value of τ evaluated based on using the experimentally obtained history of γ. In spite of the many assumptions, the model predicts the stress to some degree of accuracy. One point at which the simulation fails to accurately represent the stress is labeled on the figure by B, and is a result of a large change in the interval of data acquisition. This large change results in excessive creep in the plastic strain due to problems with the numerical integration used to obtain the plastic strain. Therefore, this is not a deficiency of the model, but a deficiency of the numerical integration.

Even though the predicted and measured results show a close similarity, the relative vertical positioning of the measured and predicted response is not as good. Since the

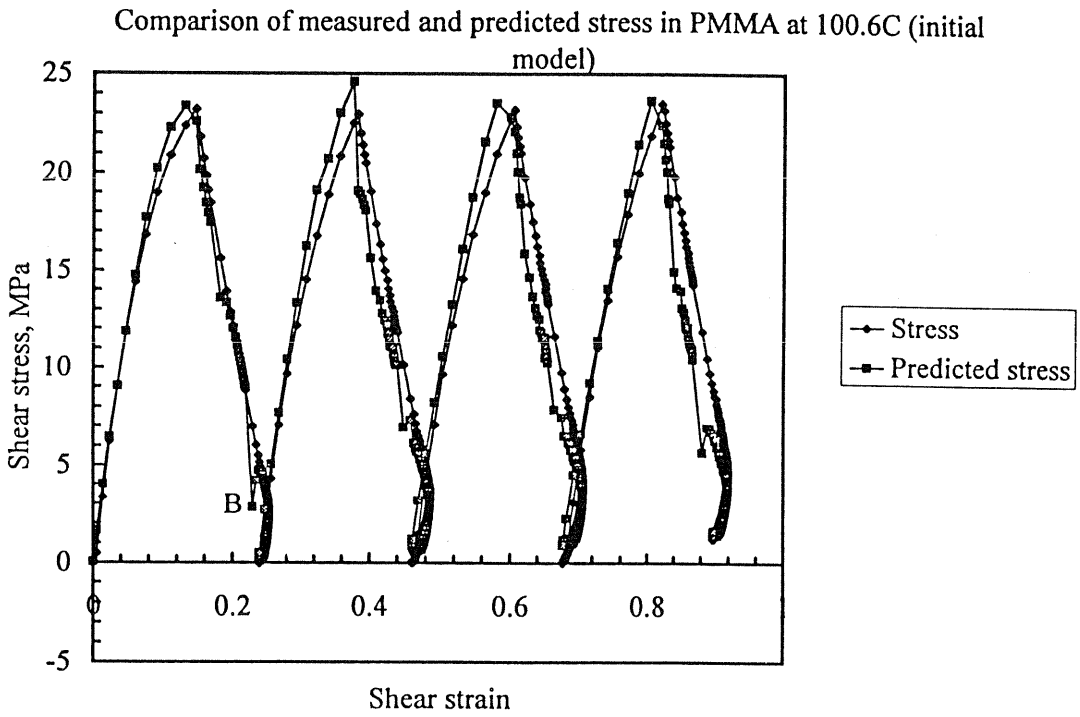

Figure 11: Comparison of the observed stress history and the predicted stress history, using the initial model for evaluating the predicted response.

horizontal positioning in the predicted response is given by experiment, the vertical positioning is what should be examined in evaluating the quality of the model.

Minor alterations of the constants can result in a much better prediction of the response. First, in evaluating the equilibrium stress it was assumed that A_1 is zero, which should result in some overestimation of the equilibrium stress. This will slightly alter the form of the model for A_3, and results in a reduction in A_1. Second, adding a slight dependence on plastic strain for the terms in the model for A_3 will result in much better predictions of the response at large plastic strains. All these alterations are easily done once the initial models developed above are complete. Figure 12 shows the comparison between the experiment and the model after the completion of these adjustments. The final form of the model, as used in Figure 12, has the following material functions at 100.6°C:

$$G = 323 - 82|\gamma^p| \quad MPa, \tag{27}$$

$$\tau^{eq} = (3.2 + 4e^{-8\gamma^{p2}})\gamma^p \quad MPa, \tag{28}$$

$$A_1 = 0.15[1 + 0.5(1 - e^{-30\gamma^{p2}})](1 - e^{-60|\gamma - \gamma^p|}), \tag{29}$$

$$A_3 = -2.8 \times 10^{-7}\{1 + (0.1 + 0.9e^{-5\gamma^p})[0.4|\rho\frac{\partial\psi}{\partial\gamma^p}| + 0.16|\rho\frac{\partial\psi}{\partial\gamma^p}|^2 + 0.192|\rho\frac{\partial\psi}{\partial\gamma^p}|^3$$

$$+ 0.0128(1.3 - 0.3e^{-10\gamma^{p2}})|\rho\frac{\partial\psi}{\partial\gamma^p}|^4]\}\rho\frac{\partial\psi}{\partial\gamma^p} \quad 1/s. \tag{30}$$

Figure 13 shows a comparison between the experimentally observed response and the predicted response in a slightly different loading. The loading consists of a rapid motion of the arm, a period at which the arm is kept fixed, rapid unloading to zero stress, and

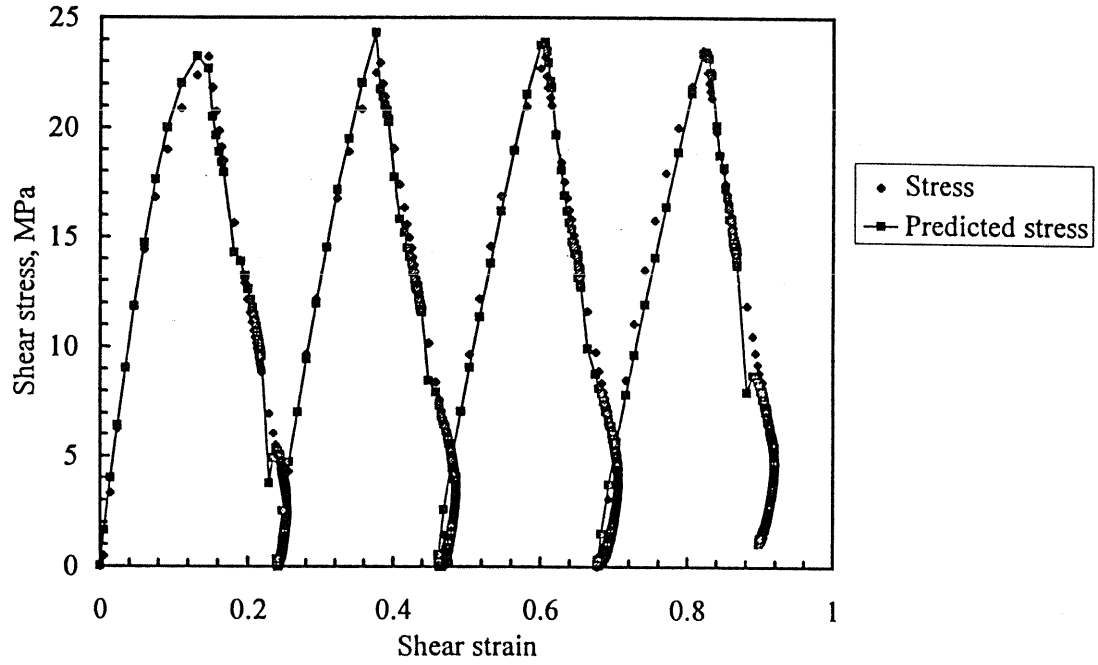

Figure 12: Comparison between the observed and predicted stress histories, using the final model for evaluating the predicted response.

a period at which the arm is fixed. This sequence is repeated over several cycles. The predicted response is based on the above material parameters and using the actual strain history as the input.

Figure 14 shows the response at constant strain rate as predicted by the model. Figure 15 shows the response at constant strain rate as observed in the experiments. The difference between these two figures is anticipated to be due to thermal heating in the actual sample, resulting in a softening of the material and the observed drop in stresses.

Figure 16 shows the predicted response of the material due to a sinusoidal strain history of amplitude 0.5 strain, and at 0.1, 1, and 10 cycles per second.

3 Preliminaries and Notation for Multidimensional Model

Before we start the multidimensional description of the constitutive model, we will lay out the notation used for this development.

In the body of this article, $\mathbf{F}$ will denote the deformation gradient, $\mathbf{F}^e$ will denote the elastic deformation gradient, and $\mathbf{F}^p$ will denote the plastic deformation gradient. These deformation gradients are assumed to be related by the multiplicative relation

$$\mathbf{F} = \mathbf{F}^e\mathbf{F}^p. \tag{31}$$

Associated with each one of the deformation gradients is a volume ratio which is evaluated

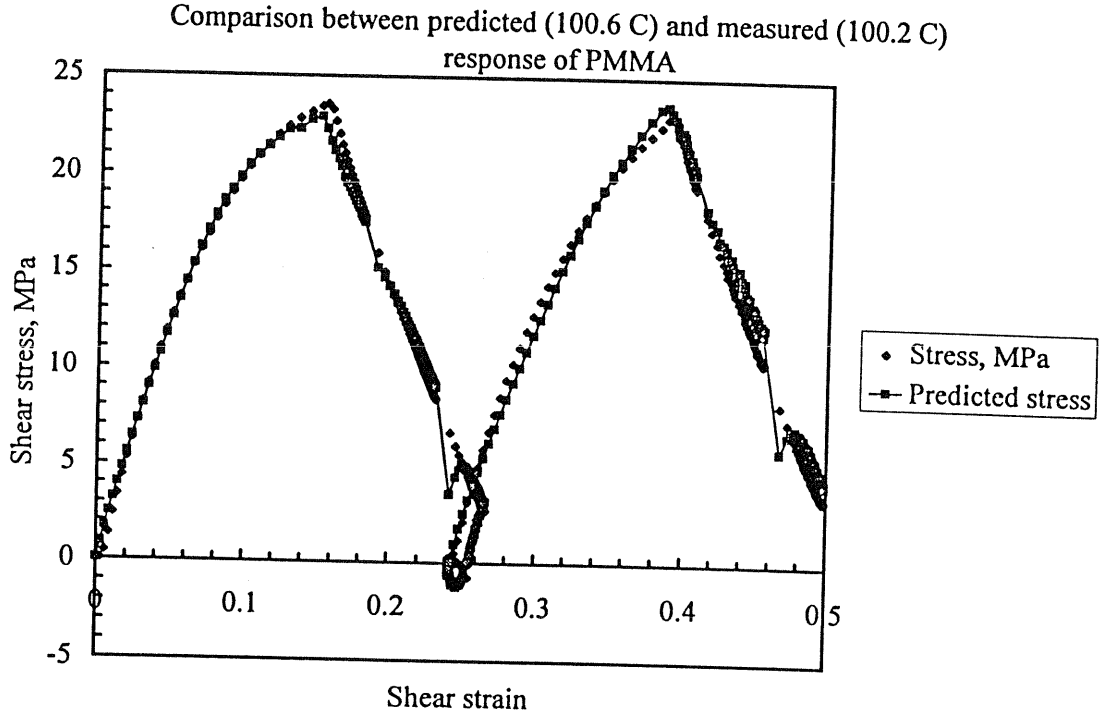

Figure 13: Comparison between the observed and predicted stress response in a second experiment.

by calculating its determinate, and denoted by

$$J = det(\mathbf{F}), \qquad J^e = det(\mathbf{F}^e), \qquad J^p = det(\mathbf{F}^p), \tag{32}$$

and they satisfy the relation $J = J^e J^p$.

The velocity gradient will be denoted by $\mathbf{L}$ and follows the relation $\mathbf{L} = \dot{\mathbf{F}}\mathbf{F}^{-1}$, where " $\dot{}$ " denotes a material time derivative and "-1" denotes the inverse.

The density will be denoted by ρ, temperature will be denoted by θ, temperature gradient will be denoted by $\mathbf{g}$, free-energy density will be denoted by ψ, entropy density will be denoted by η, and the Cauchy stress will be denoted by $\mathbf{T}$.

The entropy production inequality restricts the possible relation between the variables through the relation

$$\rho\dot{\psi} - tr(\mathbf{TL}) + \rho\eta\dot{\theta} + \frac{1}{\theta}\mathbf{q}\cdot\mathbf{g} \leq 0, \tag{33}$$

where " $\cdot$ " between two vectors represents the standard scalar product. The term $tr(\mathbf{TL}) = (\mathbf{TF}^{-T}) : \dot{\mathbf{F}}$, where the operator ":" is defined by $\mathbf{A} : \mathbf{B} = tr(\mathbf{AB}^T)$ for any two second order tensors $\mathbf{A}$ and $\mathbf{B}$, and superscript "T" denotes the transpose.

4 General Constitutive Assumptions

Our next task is to lay out basic assumptions made regarding the functional dependence of free-energy, entropy, Cauchy stress, and plastic deformation gradient. This will be

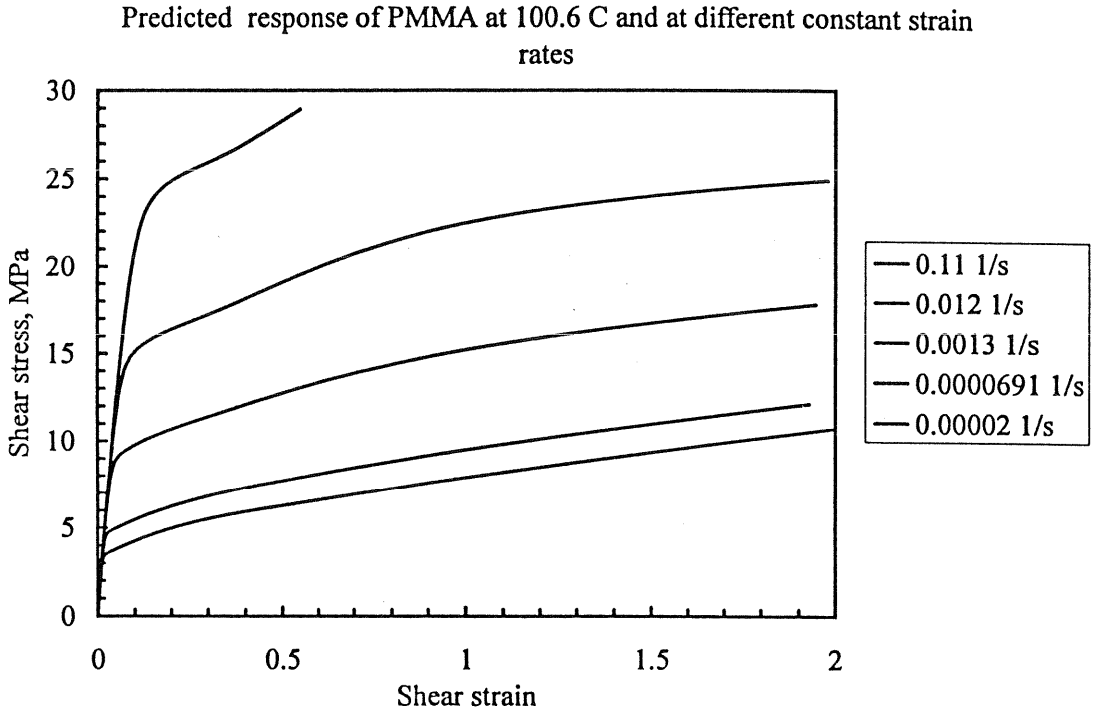

Figure 14: Predicted response for constant strain rate.

followed by more specific assumptions which should constitute the base for analyzing experimental results.

As in the model for shear, the response is characterized using a structure which borrows closely from the structure developed for plasticity, and as a result has close similarity with the model proposed by Boyce et al. (1988, 1989, 1990) and Arruda et al. (1995). The main difference between the work of these researchers and the current model is the fact that the current model is based on continuum thermodynamics, as opposed to the purely mechanical models they propose.

The free-energy, entropy, and Cauchy stress are assumed to depend on the total deformation gradient, the plastic deformation gradient, and temperature. This dependence will be written as

$$\psi = \psi^{\dagger}(\mathbf{F}, \mathbf{F}^p, \theta), \qquad \eta = \eta^{\dagger}(\mathbf{F}, \mathbf{F}^p, \theta), \qquad \mathbf{T} = \mathbf{T}^{\dagger}(\mathbf{F}, \mathbf{F}^p, \theta), \tag{34}$$

where the superscript "†" will denote the function or functional for a given variable. The heat flux is assumed to depend on the total deformation gradient, the plastic deformation gradient, temperature, and temperature gradient. This dependence will be written as

$$\mathbf{q} = \mathbf{q}^{\dagger}(\mathbf{F}, \mathbf{F}^p, \theta, \mathbf{g}). \tag{35}$$

The experimental studies of Kung and Li (1987) and Chang and Li (1988) suggest that a large portion of the stored energy is stored in the plastic volume ratio. In fact, their work suggests that more than 80% of the stored energy is stored in volumetric deformations and less than 20% is stored in other deformations. Therefore, even though the volumetric strains are small, they are very important when studying the stored energy in the polymer. To provide a theoretical mechanism to capture stored energy in volumetric distortions, the concept of a volume ratio associated with the equilibrium

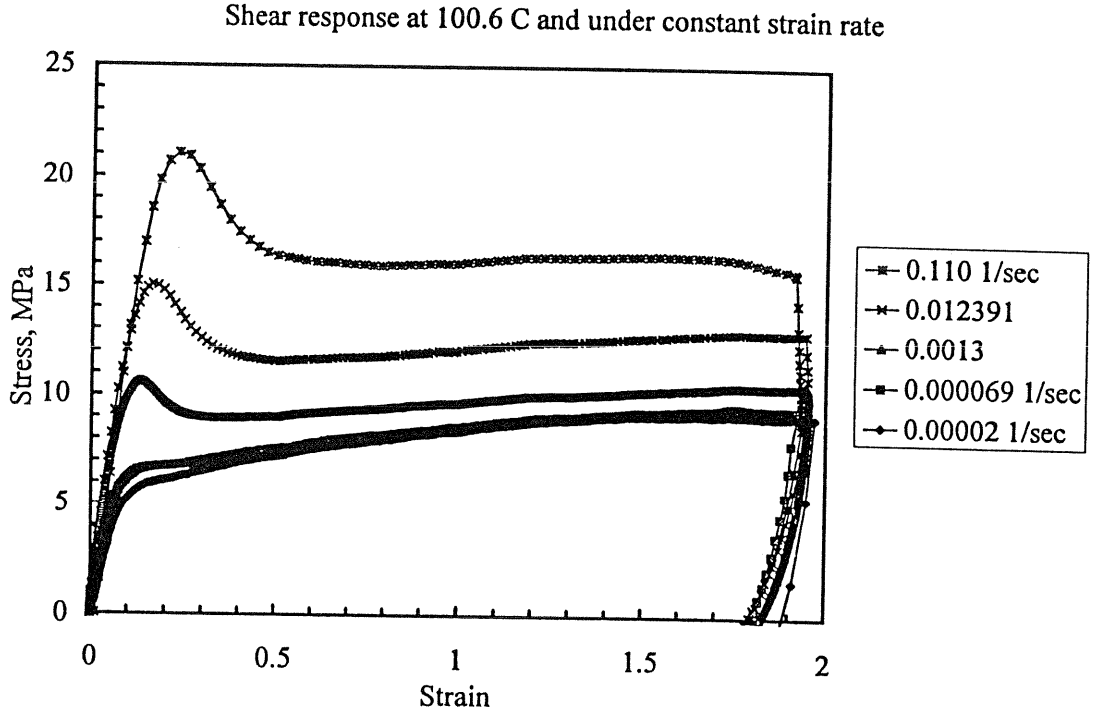

Figure 15: Observed response at constant strain rate.

response of an unloaded material will be introduced. This volume ratio will be designated by J^{eq} and will be a function only of temperature. This volume ratio will represent the volume ratio which the material will go to if it is left unloaded for an infinitely long period of time. Since the plastic deformation gradient at each instant represents the unloaded shape of the material, barring loading which could drive one away from the unloaded equilibrium state, the plastic volume ratio of the material J^p should have a tendency to migrate towards J^{eq}. This equilibrium volume ratio will be given by the relation

$$J^{eq} = J^{eq\dagger}(\theta). \tag{36}$$

The plastic flow of the material will be governed by a flow rule describing how the plastic deformation gradient changes. In view of the assumptions we have made for our one dimensional model, the following flow rule is proposed for multidimensional loading

$$\dot{\mathbf{F}}^p = \mathbf{A}_1 : \dot{\mathbf{F}} + \mathbf{A}_2\dot{\theta} + \mathbf{A}_3, \tag{37}$$

where each $\mathbf{A}_i$ is a function of $\mathbf{F}$, $\mathbf{F}^p$, and θ, and $\mathbf{A}_1$ is a fourth order tensor, and $\mathbf{A}_2$ and $\mathbf{A}_3$ are second order tensors. As was noted in the one dimensional model, this flow rule cannot be made time independent, and as a result introduces rate dependence in the model.

Introduction of (37) into the entropy production inequality (33) and following standard steps for extracting information from this inequality results in the relations

$$\mathbf{T} = \rho[\partial_{\mathbf{F}}(\psi) + \partial_{\mathbf{F}_p}(\psi) : \mathbf{A}_1]\mathbf{F}^T, \tag{38}$$

$$\eta = -\partial_\theta(\psi) - \partial_{\mathbf{F}_p}(\psi) : \mathbf{A}_2, \tag{39}$$

$$\rho\partial_{\mathbf{F}_p}(\psi) : \mathbf{A}_3 \leq 0, \tag{40}$$

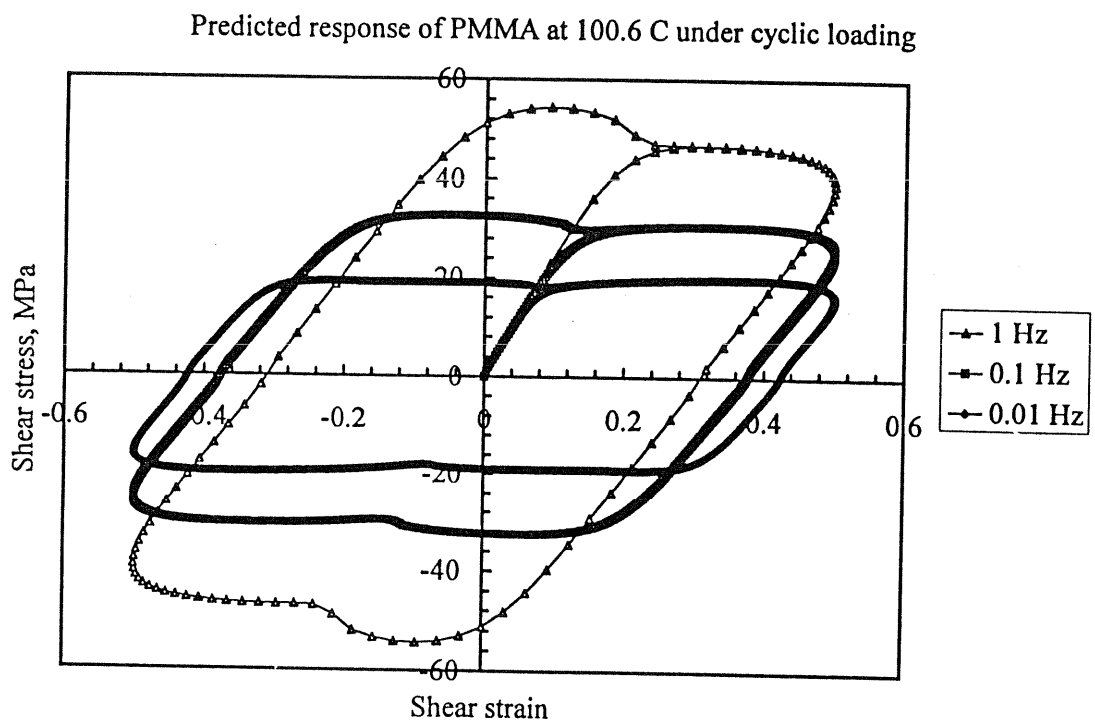

Figure 16: Predicted response for a sinusoidal strain history of amplitude 0.5 and different frequencies.

$$\rho \partial_{\mathbf{F}^p}(\psi) : \mathbf{A}_3 + \frac{1}{\theta}\mathbf{q} \cdot \mathbf{g} \leq 0, \tag{41}$$

where $\partial_{\mathbf{F}^p}(\psi)$ denotes the partial derivative of ψ with respect to $\mathbf{F}^p$. Obtaining these results requires the assumption that $\mathbf{q}$ is bounded at $\mathbf{g} = 0$.

As in the one dimensional model, the ability of the polymer to retract to its original shape without loading suggests that part of the energy expended in the deformation of the polymer is stored in a form which initiates the delayed response. Another part of the work is stored in a form which is much more readily available, resulting in an instantaneous elastic response. The remainder is dissipated by internal heating. One might suggest that on a molecular level the long term storage is associated with relocation of the chains relative to one another, while the instantaneous response is associated with small instantaneously reversible distortions of chain segments. The plastic deformation gradient will be associated with the large relocation of the chains, while the elastic deformation will be the dominant term identified with the easily reversible motion of segments.

As in the one dimensional model, the free energy will be assumed to be a combination of one term associated with the rapid elastic response and one term associated with the delayed viscoelastic recovery. This will be written as

$$\psi = \psi^e + \psi^b, \tag{42}$$

where ψ^e is associated with the instantaneous elastic response and ψ^b is associated with the delayed response. These two terms are assumed to be given by functions described as

$$\psi^e = \psi^{e\dagger}(\mathbf{F}, \mathbf{F}^p, \theta) \quad \textit{and} \quad \psi^b = \psi^{b\dagger}(\mathbf{F}^p, \theta). \tag{43}$$

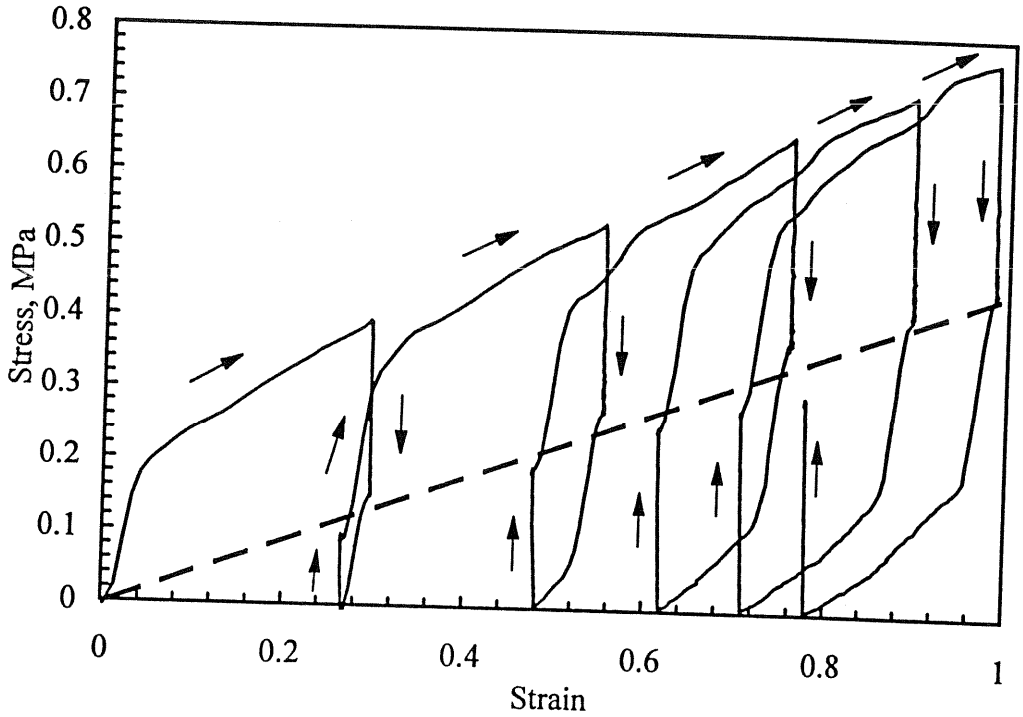

Figure 17: The attraction to an equilibrium stress as observed in an experiment on PMMA.

Since ψ^b is not a function of $\mathbf{F}$, it follows that the Cauchy stress is obtained from the relation

$$\mathbf{T} = \rho[\partial_{\mathbf{F}}(\psi^e) + \partial_{\mathbf{F}^p}(\psi^e + \psi^b) : \mathbf{A}_1]\mathbf{F}^T. \tag{44}$$

It therefore follows that the observed (measured) stress is not only a result of the local rapidly reversible distortion of chain segments, but also a function of the "back stress" (resulting from ψ^b).

The desired migration of the material towards the equilibrium volume can now be introduced into the model by introducing an energy associated with any deviations of J^p from J^{eq}. This energy would be part of the model provided for ψ^b. Equation (40) should then force $\mathbf{A}_3$ to move in the direction of eliminating this deviation. On the other hand, the speed at which the material travels towards J^{eq} is governed by the existing conditions, defined through the specific model introduced for $\mathbf{A}_3$.

The specific form of the constitutive functions must also satisfy constraints imposed by material-frame-indifference and material symmetry. If working with an annealed material, one can take advantage of the isotropy of the initial material to reduce the possible forms of the constitutive functionals. An extensive study of the effects of imposing material-frame-indifference and material symmetry on models having the structure now commonly identified with large deformation plasticity has been done by Negahban (1995).

5 Summary, Comments, and Conclusions

In this article the basic elements of a thermodynamic theory for modeling the material response of amorphous polymers around the glass transition are introduced, first through a one dimensional model for shear and later for a multidimensional model. The one dimensional model can be put in good agreement with the results of one experiment which included several loading/unloading cycles, each containing events occurring on different time scales, from several seconds to many hours.

Due to the inhomogeneous nature of shearing, shear experiments are not ideal experiments for fitting multidimensional models, yet the success in capturing all aspects of the observed response suggests that the basic ideas pursued are correct. Particularly, a modeling scheme based on plasticity, constrained by the entropy production inequality, containing an energy associated with the delayed response, and containing a flow rule as suggested is capable of predicting not only qualitatively but also quantitatively all aspects of the observed response. Namely, the fact that at sufficiently large loads the response of the polymer is characterized by stress relaxation and creep, and at sufficiently low load the response is characterized by stress buildup and recovery. In the one dimensional response, the transition between these two different types of behavior is described by a line in the stress-strain space on which the material can be held at equilibrium indefinitely. The desire of the polymer to move to this equilibrium is best seen in Figure 17 which shows that, even after several cycles of loading and unloading, every time the strain is held constant (a vertical line in the figure) the stress in the polymer either drops or increases to approach the equilibrium stress (the dashed line).

6 Acknowledgement

The author would like to thank Mr. Mark Fleming for his contributions in the design and development of the shear grips, and Mr. Nicholas Hiser for his help in preparing the manuscript and verifying the results. This work was partially supported by the National Science Foundation through grant MSS-9111895.

7 References

Arruda, E. M., Boyce, M. C., Jayachandran, R., "Effects of strain rate, temperature and thermo-mechanical coupling on the finite strain deformation of glassy polymers," *Mechanics of Materials,* vol. 19, page 193 (1995).

Boyce, M. C., Parks, D. M., Argon, A. S., "Large inelastic deformation of glassy polymers. Part I: Rate dependent constitutive model," *Mechanics of Materials,* vol. 7, pages 15-33 (1988).

Boyce, M. C., Parks, D. M., Argon, A. S., "Plastic flow in oriented glassy polymers," *International Journal of Plasticity,* vol. 5, pages 593-615 (1989).

Boyce, M. C., Arruda, E. M., "An experimental and analytical investigation of the large strain compressive and tensile response of glassy polymers," *Polymer Engineering and Science,* vol. 30, no. 20, pages 1288-1298 (1990).

Chang, B. T.-A., Li, J. C. M., "Stored energy of cold work in polystyrene," *Polymer Engineering and Science,* vol. 28, no. 18, pages 1198-1202 (1988).

Kung, T.-M., Li, J. C. M., "Recovery processes in amorphous polymers," *Journal of Materials Science,* vol. 22, pages 3620-3630 (1987).

Negahban, M., "A study of thermodynamic restrictions, constraint conditions, and material symmetry in fully strain space theories of plasticity," *International Journal of Plasticity,* (in press).